Proceedings of the 21st ICSMGE, Vienna, Austria, 14 – 19 June 2026. Pistrol, Adam & Schweiger (eds.)
Published by: ÖGG, Austrian Society for Geomechanics, Salzburg, Austria, ISBN 978-3-9503898-4-5
https://doi.org/10.53243/ICSMGE2026-1227

Pullout Experiments for Field Testing of Soil-Nail Interface Seismic Behavior.

Ghida Hawwa, Jean de Sauvage, Jean-Pierre Rajot, Yannick Fargier, Patrick Joffrin
Université Gustave Eiffel, Bron, France, ghida.hawwa2@univ-eiffel.fr.

ABSTRACT: Soil nailed walls are very resilient to seismic loading and the reason of this remarkable performance is still not fully understood. Several researches have been done focusing on the full structure stability by means of shaking table and centrifuge tests. Yet, an important factor of the performance of soil nailed walls lies in the energy dissipated through friction at the interface between soil and nail upon the deformation of the reinforced mass during construction phases. The properties of this interface including its stiffness are thus to be accounted for locally. In the following paper, field dynamic pullout tests are presented, carried out through of newly developed dynamic pullout device, allowing to impose loads of predefined frequencies. The interface is monitored with optical fiber that allows to track deformations, and eventually displacements locally all along the bar of reinforcement. The tests investigate two different types of soil, and different frequencies of solicitations.

KEYWORDS: Soil-nailed wall, pull out test, friction law, seismic behavior.

1 INTRODUCTION

Soil nailing, introduced in France in the early 1970s, is widely used to improve in-situ soil stability. Its popularity stems from adaptability, efficient construction with lightweight equipment, and cost-effectiveness (Schlosser and Unterreiner, 1991). These systems stabilize slopes and excavations by mobilizing tensile forces in the nails as surrounding soil deforms. Their performance depends largely on the soil–nail interface, where axial forces transfer through friction and adhesion along the nail length. (Bruce and Jewell, 1986).

The excellent seismic performance of soil-nailed walls has been observed in real events, such as the 1989 Loma Prieta earthquake, where multiple walls—some located near the epicenter—showed no signs of distress despite widespread structural damage nearby (Vucetic, Tufenkjian and Felio, 1998). These observations have spurred interest in understanding their dynamic behavior.

Static pull-out tests have been widely used to explore this mechanism, examining the influence of nail geometry, stiffness, interface roughness, and soil characteristics through different laboratory scale tests as in the work of Shahraki Ghadimi et al., (2017) and (Su, 2006). Full scale pullout tests as well were investigated through the French National Project Clouterre (Schlosser, 1989) and the project carried by (Hong et al., 2013) as well as Lum, (2007). These field-scale experiments have provided essential benchmarks for design under static conditions, yet offer limited insight into dynamic interface mechanisms.

Dynamic responses have been studied using several approaches: centrifuge modeling captures scaled seismic response; 1g shaking tables provide insight into full-structure behavior under controlled excitation; and numerical models simulate soil-structure interaction under varying seismic intensities. The investigations have been carried out experimentally through centrifuge tests as in the work of Tei, (1993) and Tufenkjian and Vucetic, (2000), or through 1g shaking table experiments as has been studied in the research of Yazdandoust, (2017),Xu, Hatami and Jiang, (2020) and Giri and Sengupta, (2009).Other research involved numerical studies as in the studies presented by Chavan, Mondal and Prashant, (2017),Moniuddin, Manjularani and Govindaraju, (2016) and Koseki et al.,(2006) .

Most of these investigations have focused on the overall structural response, studying different parameters of design without capturing the detailed interaction at the interface level. (Tan et al., 2008)investigated the rapid pullout behavior of soil nails using a mechanical impulse system generating tensile loads at ~35 Hz. Their results showed stiffer pre-peak responses and higher pullout capacities than quasi-static tests, particularly for rough, large-diameter nails, with enhanced interface stiffness under rapid loading. However, this approach provided limited insight into full strain evolution along the nail.

To address this, a novel dynamic pullout setup was developed at the GERS-RRO laboratory, enabling controlled harmonic tensile loads while monitoring distributed strains via embedded optical fibers. Field tests were conducted to assess the system's performance and examine interface behavior, with findings aimed at improving dynamic soil–nail interaction models and seismic design reliability.

2 EXPERIMENTAL SETUP

2.1 *Field Geological Condition*

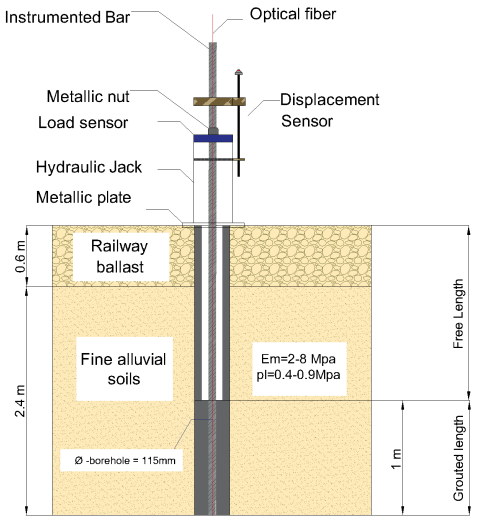

Figure 1. Illustration of the soil conditions as well as the instrumentation of the installed setup.

To replicate real installation conditions, the tests were conducted in the field at the SNCF station of l'Arbresle, on a site dedicated to extending the train repair/parking area. Soil reinforcement with micro-piles was carried out by NGE Fondation. Geological investigation showed a homogeneous alluvial deposit with the water table at 8 m depth. Soil properties determined through pressure meter test and are indicated in Figure 1.

2.2 *Pullout Machine*

A new portable hydraulic device was developed to apply controlled dynamic tensile loads to reinforcement bars in geotechnical structures. It comprises five lightweight (<30~kg) components forming a hydraulic circuit with a 700~bar pump and a 600~kN jack, all managed by a programmable controller. The system can superimpose a dynamic pulse (0.1–5~Hz, up to 50\% of the static load) on a static tensile load applied either incrementally or linearly, enabling both laboratory and field testing. The hydraulic circuit forming the machine is presented in Figure 2.

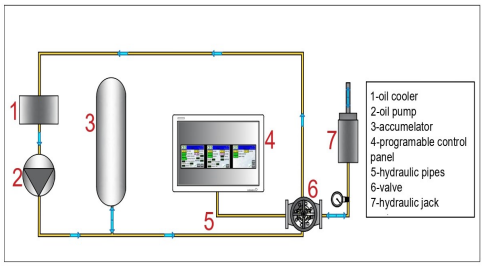

Figure 2. Schematic representation of the hydraulic circuit constituting the pullout machine.

2.3 *Instrumentation and Monitoring*

Three SAS 500/550 MPa bars (yield 405 kN) were tested. Two 4 m-long, 32 mm-diameter bars were instrumented with 2 m optical fibers connected to a LUNA ODiSI 6000 (80 Hz, 2.6 mm resolution). Each nail had a 600 kN load cell, pressure gauge, and displacement sensor, and was installed in 3 m-deep, 115 mm boreholes spaced 1 m apart. The 1 m bar section above ground was reserved for instrumentation (Figure 1). The sealed length was set to 1.0 m to ensure sufficient friction mobilization within the proximal bonded zone while keeping the response representative of field-scale soil–nail interaction under dynamic loading. This length allows local interface behavior to be captured.

3 EXPERIMENTAL PROGRAM

The program included one test per bar: a static pullout on the non-fibered bar, and two dynamic tests on the instrumented bars to assess frequency effects.
A 1D finite element simulation with ANCRAGE (Rajot, 2023) was used to define the static test protocol. The software models axial load transfer between soil and passive reinforcements via shear stress–displacement laws, requiring soil profile (from pressuremeter tests), inclusion properties, interface stiffness kτ, and unit skin friction qs. For fine soils, kτ was estimated from the Menard modulus Em as:

$$k_\tau = \frac{2E_m}{D} = 1.1 \times 10^5\ kPa/m \qquad (1)$$

Unit skin friction (q_s) was estimated using the Abaqus provided by the CLOUTERRE project (Schlosser, 1989) by *200 kPa* . The limit pullout force is then determined at 168 kN.

3.1 *Test protocol*

Once the pullout force is estimated, the static pullout test was carried to validate the capacity of the nails installed, and then to prepare the dynamic test protocol. For the static test, the incremental load (steps) configuration is defined, where three steps of 65,114 and 168 kN each of 20 min duration were defined. The traction force is validated to be less than 85% of the yielding load (that is 340 kN). The nail was then pulled out at 168 kN, which validates the values simulated numerically. Based on this observation, the dynamic protocol is defined in the Table 1 below:

Table 1. Dynamic test protocol on instrumented bars

Test	Static Load		Dynamic load	
	Loading level (%$F_{pullout}$)	Load (kN)	Frequency (Hz)	Amplitude (%)
DYN-2	50%	87	2	15
DYN-4	70% 100%	120 168	4	15

Each of the loading steps was defined for 15 min, and the dynamic pulse superposed on each was centered in the step for 10 sec of loading). A preliminary static loading step at a low force level (around 10 % of pullout force) was applied prior to the dynamic test to ensure the stability of the setup, and consistent initial conditions.

4 RESULTS AND DISCUSSION

4.1 *Loads and Displacements*

The tests were carried out according to the defined protocol above. The bar under test DYN-2 was pulled out at force of 168 kN, corresponding to the same value of that of static pullout force. For the second bar however under test DYN-4, pullout failure was not reached until tension of 200 kN. Thanks to the optical fiber, the strains along the nails' length are measured and presented in Figure 3.

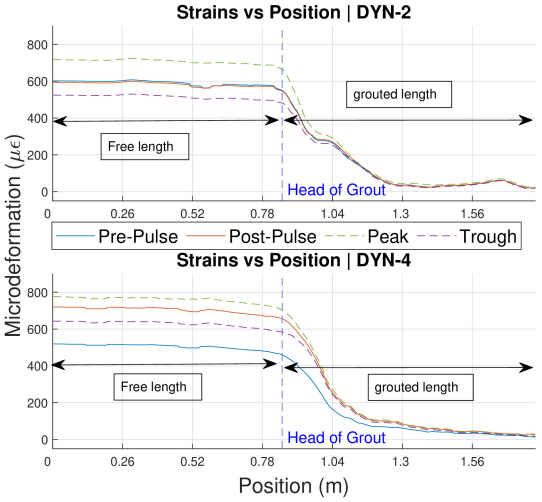

Figure 3.Measured strains at different instants along nail's length for loading level of 87 kN.

The grouted region is the part of the nail subjected to contact with the surrounding soil, and eventually the part experiencing friction. From the strains, the axial loads at each position can thus be calculated according to equation (2):

$$T_i = E.\frac{\pi D^2}{4}.\varepsilon_i \qquad (2)$$

Where T_i is the tension at gauge i, E is the Young modulus of steel, D is diameter of the used bar and ε_i corresponds to the measured strain at gauge i. The axial loads along the grouted part of the nail for the first loading step are thus plotted in Figure 4 . It can be seen that the axial loads vary nonlinearly

along the interface, indicating that the mobilized resistance varies with location, which can be attributed to the non-uniform nature of the load transfer mechanism, emphasizing thus the necessity of understanding the local behavior along the interface during dynamic loading. The displacements were calculated by integrating the measured strains along the defined gauge length, in this case 2.6 mm. from the measured strains, with a boundary condition of displacement at nail's end is $u_{(f)}$=0 mm, where *f* correspond to the final gauge of the optical fiber. This assumption is made due to the very low strains measured at that part of the nail (in order of 10με).

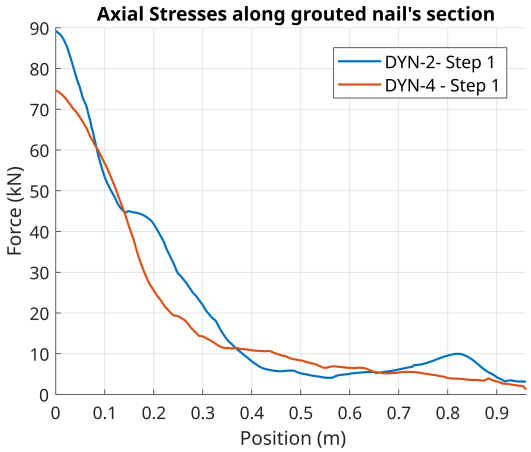

Figure 4. Axial loads computed from measured strains along the grouted part of the nail.

4.2 *Stiffness of Interface*

The interface stiffness can be defined by the resistance offered by the contact zone between the soil and the inclusion element to relative displacement or deformation. It quantifies how much force is required to cause a mobilization of the displacement at the interface, representing the mechanical interaction and load transfer capacity across that boundary. The interface stiffness is then computed along the full interface of the grouted nail. In order to understand how the dynamic loading affects the interface stiffness, and due to the process in which the dynamic load is defined in these tests (superposition of the dynamic pulse on the static tension), the dynamic interface stiffness is calculated according to equation (3), with T being the axial load and δ the displacement , with static and dynamic instants being marked in Figure 5 .

$$k_{dynamic} = \frac{|T_{dynamic} - T_{static}|}{|\delta_{dynamic} - \delta_{static}|} \quad (3)$$

For each test, the interface dynamic stiffness is calculated. To isolate the influence of dynamic loading effects, this dynamic stiffness is normalized with respect to the static interface stiffness, which corresponds to the quasi-static loading conditions applied just before the dynamic pulse. This normalization allows for a clearer interpretation of how dynamic excitation alters the interface behavior independently of the baseline static response. The comparative results are illustrated in Figure 6.

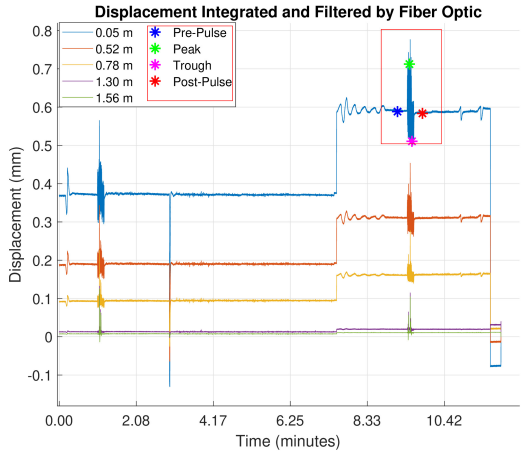

Figure 5. Schematic representation of the targeted instants for computing the dynamic interface stiffness.

Mobilized displacements along the soil–nail interface was larger in the 2 Hz test (DYN-2) than in the 4 Hz test (DYN-4). Correspondingly, the normalized interface stiffness was higher at 4 Hz, especially near the nail head for displacements above 0.004 mm. This indicates that increasing excitation frequency enhances interface stiffness due to more constrained movements and rate-dependent soil behavior. Higher frequencies correspond to faster loading rates, where the load variation with displacement and time becomes critical, linking the excitation frequency directly to the rate effect on the interface response. static load to the peak load is inversely proportional to the frequency.

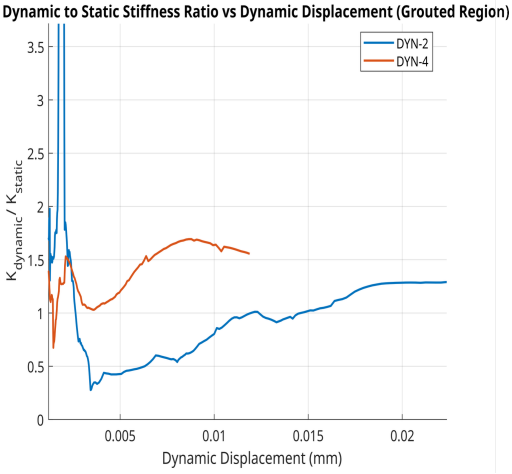

Figure 6. Ratio of dynamic to static stiffness vs displacements along the grouted region of the nail.

This means that the time required to mobilize a given amount of load is shorter at higher excitation frequencies than at lower ones, ultimately resulting in higher loading rates. The experimental findings from this study align well with the observations reported by (Tan et al., 2008) who investigated the pullout behavior of soil nails subjected to rapid loading at a frequency of approximately 35 Hz in dry sand, in comparison to quasi-static loading conditions. The results showed a clear enhancement in pre-peak pull-out response, with greater shaft stiffness under dynamic loading. This indicates rate-dependent behavior of the soil–nail interface, where apparent stiffness increases with loading rate. the fact that, under dynamic

excitation, the shaft resistance (or mobilized shear resistance along the interface) can be decomposed into two key components: (1) a displacement-dependent component, representing the classic mobilization of friction and interface shear with increasing relative movement, and (2) A rate-dependent component, which becomes significant under rapid loading and reflects the influence of radiation damping effects. The rate-dependent component is closely associated with what is known as radiation damping, a phenomenon where energy is dissipated through wave propagation into the surrounding medium. This effect is particularly pronounced in the nonlinear, low-confinement zone adjacent to the shaft, where the zone experiences large strains, and relative velocity to that of the outer field, which is considered undisturbed. This concept was investigated by different researches investigating the axial dynamic behavior of piles as in the studies of (Novak, 1974),Nogami, Asce and Konagai, (1987), El Naggar and Novak (1994) , and Tu, El Naggar and Wang (2022) ,

5 CONCLUSIONS

This research aimed to investigate the influence of dynamic loading on the behavior of the soil–nail interface. To achieve this, a novel experimental setup was developed, combining a custom-designed dynamic pullout testing system capable of applying predefined dynamic pulses at various frequencies, and an optical fiber monitoring system enabling full-length, localized measurements along the interface. The study presents results from field-scale dynamic pullout tests conducted under different excitation frequencies. The performance of the developed machine proved to be reliable and effective, enabling controlled dynamic loading and high-resolution data acquisition. The behavior of the soil–nail interface was observed to be nonlinear, particularly under dynamic loading. A detailed investigation of the interface stiffness revealed that stiffness increases with higher loading rates (i.e., higher excitation frequencies). This trend is consistent with findings from previous research and may be attributed to the effects of radiation damping and rate-dependent soil behavior, particularly within the zone adjacent to the nail.To build on these results, further tests are planned under varying site conditions and loading frequencies to develop a broader comparative basis. Additionally, a back-analysis will be carried out using existing theoretical models to validate and further interpret the experimental findings.

6 ACKNOWLEDGEMENTS

The authors would like to acknowledge the support provided by the technical team of RRO-GERS laboratory team. In addition, a special thanks to the team of NGE FONDATION for their aid and support on providing the site for the tests, and carrying the installation procedure.

7 REFERENCES

Bruce, D.A. and Jewell, R.A., 1986. *Bruce: Soil nailing: application and practice-part 1 - Google Scholar*. Available at: <https://scholar.google.com/scholar_lookup?&title=Soil%20nailing%3A%20application%20and%20practice%20-%20part%201&journal=Ground%20Engineering&volume=19&issue=8&pages=10-15&publication_year=1986&author=Bruce%2CDA&author=Jewell%2CRA> [Accessed 6 April 2023].

Chavan, D., Mondal, G. and Prashant, A., 2017. Seismic analysis of nailed soil slope considering interface effects. *Soil Dynamics and Earthquake Engineering*, 100, pp.480–491. https://doi.org/10.1016/j.soildyn.2017.06.024.

El Naggar, M.H. and Novak, M., 1994. Nonlinear Axial Interaction in Pile Dynamics. *Journal of Geotechnical Engineering*, 120(4), pp.678–696. https://doi.org/10.1061/(ASCE)0733-9410(1994)120:4(678).

Giri, D. and Sengupta, A., 2009. Dynamic Behavior of Small Scale Nailed Soil Slopes. *Geotechnical and Geological Engineering*, 27(6), pp.687–698. https://doi.org/10.1007/s10706-009-9268-x.

Hong, C.-Y., Yin, J.-H., Pei, H.-F. and Zhou, W.-H., 2013. Experimental study on the pullout resistance of pressure-grouted soil nails in the field. *Canadian Geotechnical Journal*, 50(7), pp.693–704. https://doi.org/10.1139/cgj-2012-0103.

Koseki, J., Bathurst, R., Guler, E., Kuwano, J. and Maugeri, M., 2006. *Seismic stability of reinforced soil walls*.

Lum, W.C.W., 2007. STATIC PULLOUT BEHAVIOUR OF SOIL NAILS IN RESIDUAL SOIL.

Moniuddin, Md.K., Manjularani, P. and Govindaraju, L., 2016. Seismic analysis of soil nail performance in deep excavation. *International Journal of Geo-Engineering*, 7(1), p.16. https://doi.org/10.1186/s40703-016-0030-y.

Nogami, T., Asce, M. and Konagai, K., 1987. Dynamic Response of Vertically Loaded Nonlinear Pile Foundations.

Novak, M., 1974. Dynamic Stiffness and Damping of Piles.

Rajot, J.-P., 2023. Analyse de l'interaction axiale des ancrages et autres inclusions linéiques dans les sols et les roches Version 1.0.

Schlosser, F., 1989. LE PROJET NATIONAL CLOUTERRE. *ANNALES DE L'INSTITUT TECHNIQUE DU BATIMENT ET DES TRAVAUX PUBLICS*, [online] (473 (QG179)). Available at: <https://trid.trb.org/view/1021811> [Accessed 6 April 2023].

Schlosser, F. and Unterreiner, P., 1991. Soil Nailing in France: Research and Practice.

Shahraki Ghadimi, A., Ghanbari, A., Sabermahani, M. and Yazdani, M., 2017. Effect of soil type on nail pull-out resistance. *Proceedings of the Institution of Civil Engineers - Ground Improvement*, 170(2), pp.81–88. https://doi.org/10.1680/jgrim.15.00038.

Su, L., 2006. Laboratory pull-out testing study on soil nails in compacted completely decomposed granite fill. [online] Available at: <https://theses.lib.polyu.edu.hk/handle/200/2652> [Accessed 17 February 2023].

Tan, S.A., Ooi, P.H., Park, T.S., Cheang, W.L. and Professor, A., 2008. Rapid Pullout Test of Soil Nail.

Tei, K., 1993. *A study of soil nailing in sand*. [http://purl.org/dc/dcmitype/Text] University of Oxford. Available at: <https://ora.ox.ac.uk/objects/uuid:3987e4e6-e623-4764-beb3-35feb9f4cb4b> [Accessed 9 June 2023].

Tu, Y., El Naggar, M.H. and Wang, K., 2022. Nonlinear fictitious-soil pile model for pile high-strain dynamic analysis. *Soil Dynamics and Earthquake Engineering*, 162, p.107464. https://doi.org/10.1016/j.soildyn.2022.107464.

Tufenkjian, M.R. and Vucetic, M., 2000. Dynamic Failure Mechanism of Soil-Nailed Excavation Models in Centrifuge. *Journal of Geotechnical and Geoenvironmental Engineering*, 126(3), pp.227–235. https://doi.org/10.1061/(ASCE)1090-0241(2000)126:3(227).

Vucetic, M., Tufenkjian, M.R. and Felio, G.Y., 1998. *The Loma Prieta, California, earthquake of October 17, 1989–earth structures and engineering characterization of ground motion*. Earth structures and engineering characterization of ground motion. [online] Washington: U.S. G.P.O. Available at: <https://catalog.hathitrust.org/Record/011195881> [Accessed 30 January 2023].

Xu, P., Hatami, K. and Jiang, G., 2020. Study on seismic stability and performance of reinforced soil walls using shaking table tests. *Geotextiles and Geomembranes*, 48(1), pp.82–97. https://doi.org/10.1016/j.geotexmem.2019.103507.

Yazdandoust, M., 2017. Experimental study on seismic response of soil-nailed walls with permanent facing. *Soil Dynamics and Earthquake Engineering*, 98, pp.101–119. https://doi.org/10.1016/j.soildyn.2017.04.009.